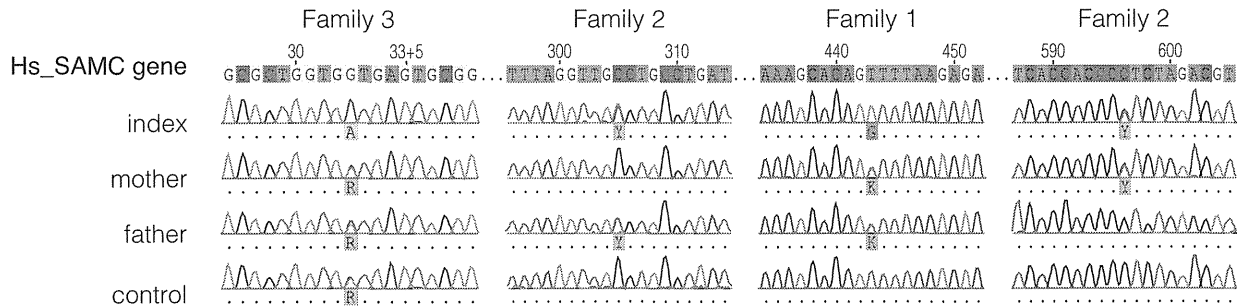
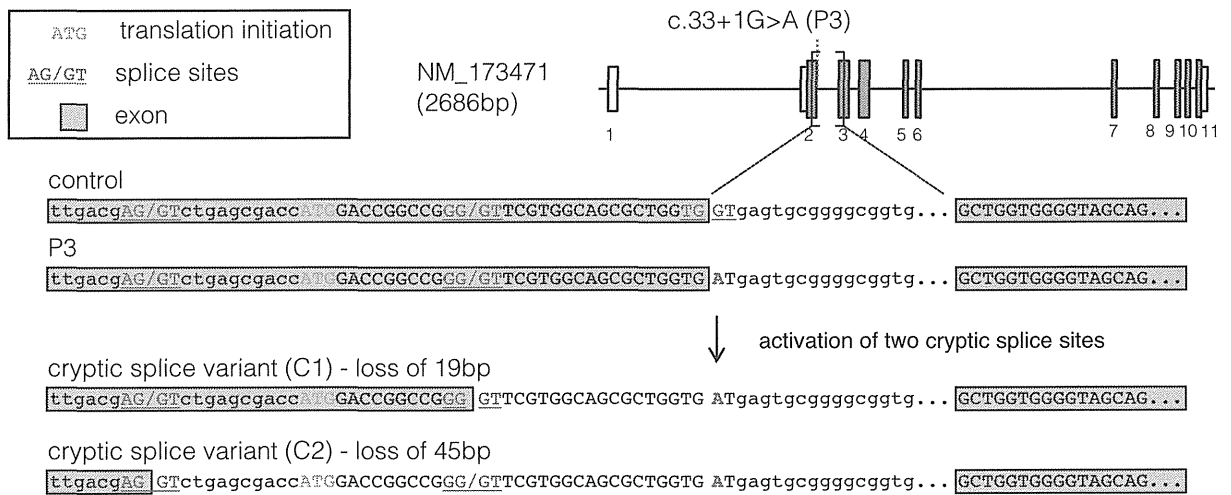


Figure S1: Bioenergetic analyses of mitochondria and muscle histology from individuals P1 and P2. **A)** Mitochondrial ATP production rate (MAPR) was determined by a firefly luciferase-based method at 25°C, using six different substrate combinations (Glu = glutamate; Succ = succinate; Mal = malate; TMPD = N,N,N',N'-Tetramethyl-p-phenylenediamine dihydrochloride; Asc = ascorbate; Pyr = pyruvate; PalCar = palmitoyl-L-carnitine; Rot = rotenone). Results are presented as the ATP synthesis rate (units) per unit of citrate synthase (CS) activity (control n=11; age 0–5 years). **B)** Respiratory chain enzyme activities of complex I (NADH:coenzyme Q reductase), complexes I and III (NADH:cytochrome c reductase), complex II (succinate dehydrogenase), complexes II and III (succinate:cytochrome c reductase, SCR), complex IV (COX) and CS were determined. Results are presented as percentage of mean control (n=9; age 0–5 years) values. The range of control values is depicted as \pm SD. **(C)** cytochrome c - succinate dehydrogenase (COX-SDH) double staining of skeletal muscle from P1. **(D)** Blue-native PAGE followed by Western blot analysis of control (C1), individual with isolated complex I defect (CO I) and P1 skeletal muscle mitochondria. Antibodies against complex I, complex III and complex IV were used. **(E)** Respiratory chain enzyme activities as in **(B)** on P2 muscle mitochondria. **(F)** Cytochrome oxidase (COX) staining of skeletal muscle from 3 years old P2.

A)



B)



C)

| Isoform | splice site used | % of clones identified (n=48) | |
|---------|----------------------------|-------------------------------|---------------|
| | | control | individual P3 |
| P.1 | wild type consensus | 63.5 | 0 |
| P.1 | cryptic splice site 1 (C1) | 0 | 31.2 |
| P.1 | cryptic splice site 2 (C2) | 0 | 54.2 |
| S.1 | wild type consensus | 36.5 | 0 |
| S.1 | cryptic splice site 1 (C1) | 0 | 0 |
| S.1 | cryptic splice site 2 (C2) | 0 | 10.5 |
| S.1 | other* | 0 | 4.1 |

* two other splice isoforms of downstream regions following the UTR of the shorter isoform (S.1) were detected.

Figure S2: Electropherogram from Sanger sequencing results aligned to *SLC25A26*. (A) Fibroblast or blood DNA from family members were used for Sanger sequencing of *SLC25A26* (NM_173471.3). Control sample of family 1 is the unaffected sibling. (B) Schematic diagram showing the cryptic splice variants generated by the c.33+1G>A mutation in P3. (C) Cloning and sequencing of *SLC25A26* splice variants C1 and C2. PCR products from cDNA from control and P3 fibroblasts were cloned into pCRII TOPO vector (Invitrogen) and sequenced to determine the appropriate splice variant. Total number of clones sequenced (n=48).

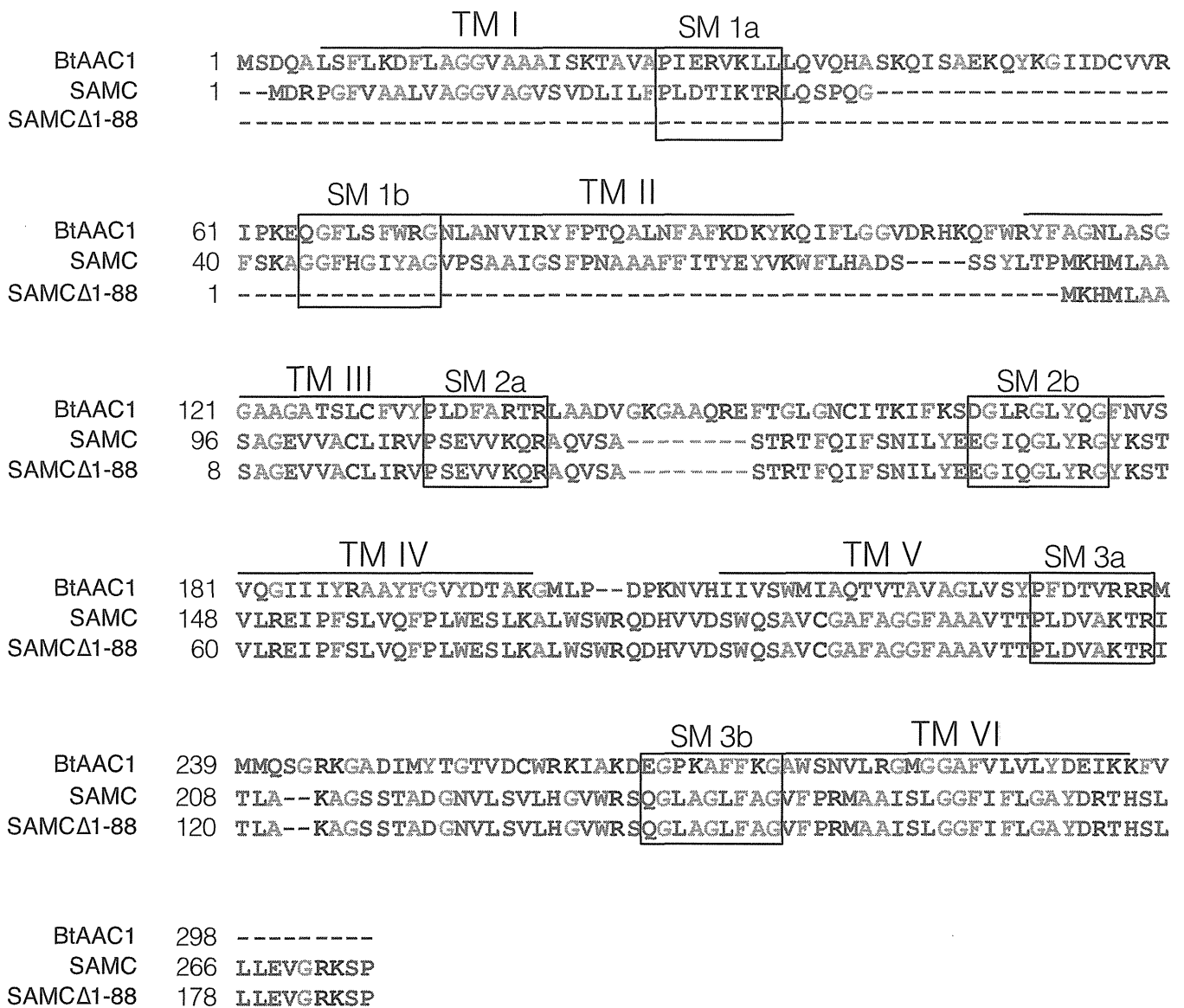


Figure S3. Alignments of the bovine ADP/ATP carrier (BtAAC1), SAMC and SAMCΔ1-88. The six transmembrane α -helices (TM I - TM VI) are linked by hydrophilic segments. The three signature motifs (SM1-SM3) present in the primary structure of the mitochondrial carriers are highlighted.

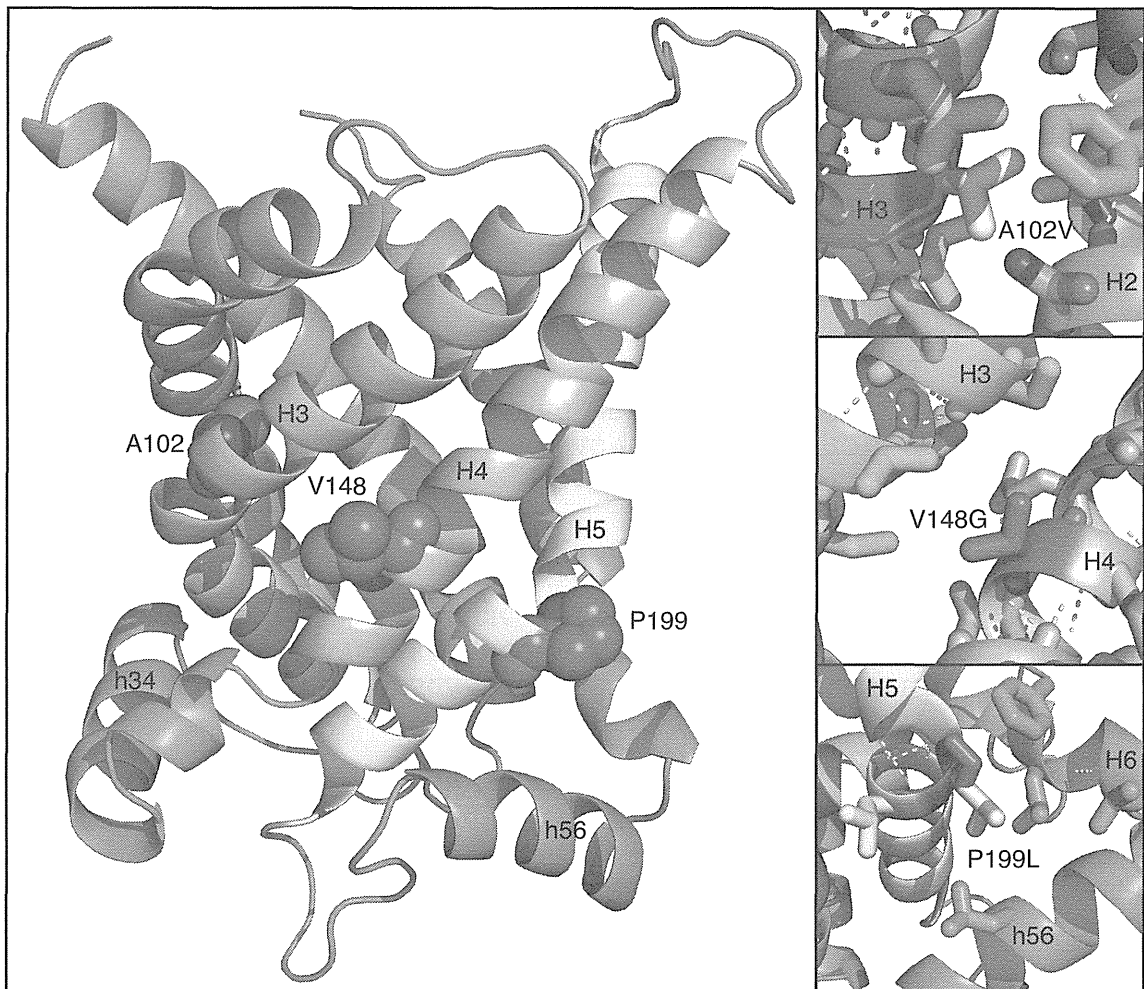


Figure S4: Structural homology model of SAMC illustrating the position of the p.Ala102Val, p.Val148Gly and p.Pro199Leu mutations. The homology model of human SAMC was made with MODELLER by using the carboxyatractyloside-inhibited ADP/ATP carrier structure (PDB ID 1OKC) as a template. The left panel shows the SAMC homology model in cartoon from a lateral view in the membrane plane with transmembrane α -helices H3, H4 and H5 in cyan, orange and yellow, respectively, and the rest of the molecule in green. The mutated residues are shown as spheres in magenta. The right panels show the mutated residues (magenta) and the replacing residues present in the SAMC mutants (white) as sticks at their positions. A102 is located at the interface between transmembrane α -helices H2 and H3. The side chain of V148 protrudes from transmembrane α -helix H4 towards the membrane. P199 creates a kink in transmembrane α -helix H5 in the cytoplasmic conformation of the carrier and its side chain is positioned towards matrix α -helix h56 and transmembrane α -helix H6.

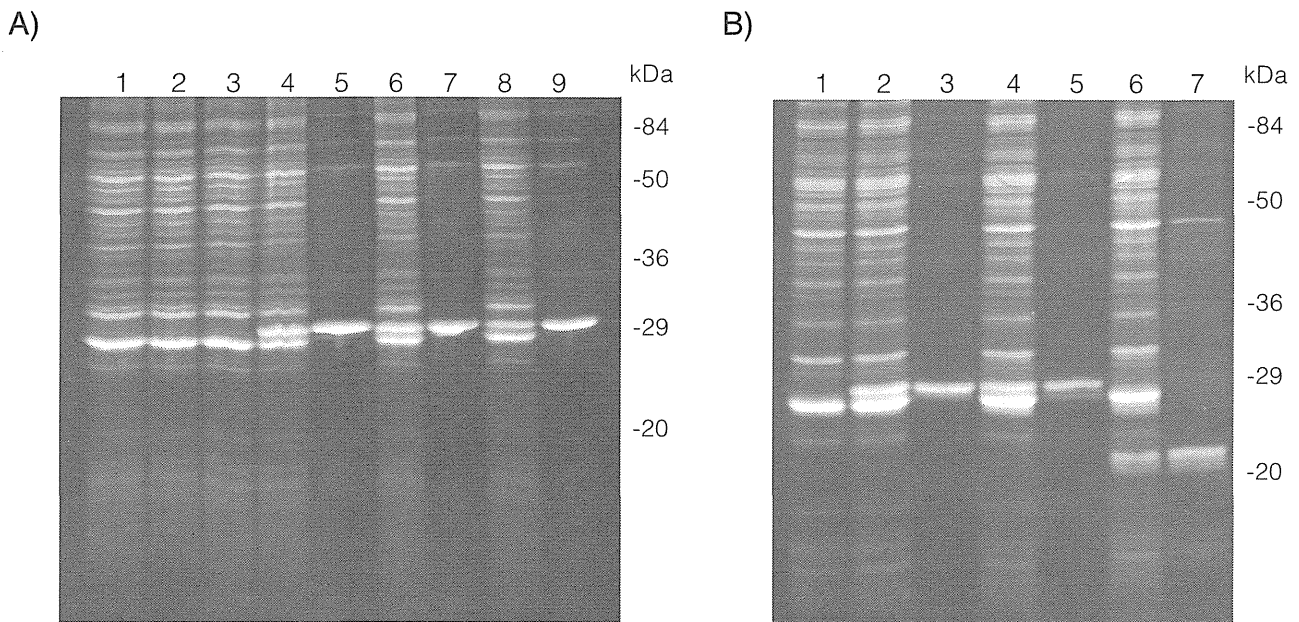


Figure S5. Expression of wild-type and SAMC variants in *E. coli* and their purification. (A) Protein extracts from *E. coli* expressing control (BL-21 CodonPlus(DE3)-RIL expression vector) (lanes 1,3), wild-type (lanes 2, 4-5), p.Ala102Val (lanes 6-7) and p.Val148Gly (lanes 8-9) SAMC were separated by SDS PAGE and stained with Coomassie Blue. Samples were taken before (lanes 1 and 2) or 5h after (lanes 3, 4, 6 and 8) induction. Lanes 5, 7 and 9 represent purified SAMC (6.2 μ g), p.Ala102Val SAMC (4.3 μ g) and p.Val148Gly SAMC (4.7 μ g) derived from bacteria shown in lanes 4, 6 and 8, respectively. (B) Protein extracts from *E. coli* expressing control (BL-21 CodonPlus(DE3)-RIL expression vector) (lane 1), wild-type (lanes 2-3), p.Pro199Leu (lanes 4-5) and SAMC Δ 1-88 (lanes 6-7) were analyzed as above. Samples were collected 5h after (lanes 1, 2, 4 and 6) induction. Purified samples for SAMC (3.6 μ g), p.Pro199Leu SAMC (2.5 μ g) and SAMC Δ 1-88 (3 μ g) derived from bacteria shown in lanes 2, 4 and 6 are shown in lanes 3, 5 and 7, respectively.

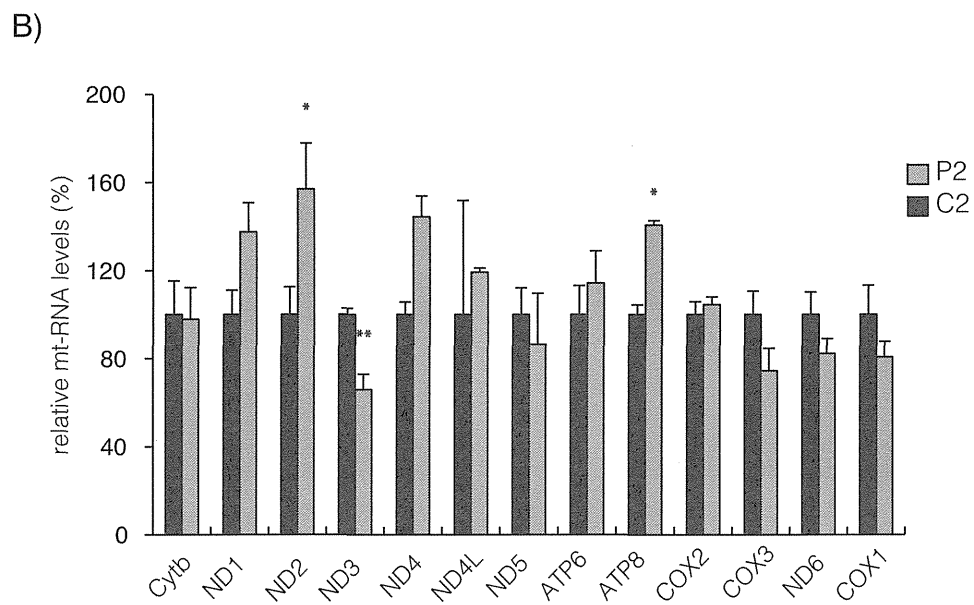
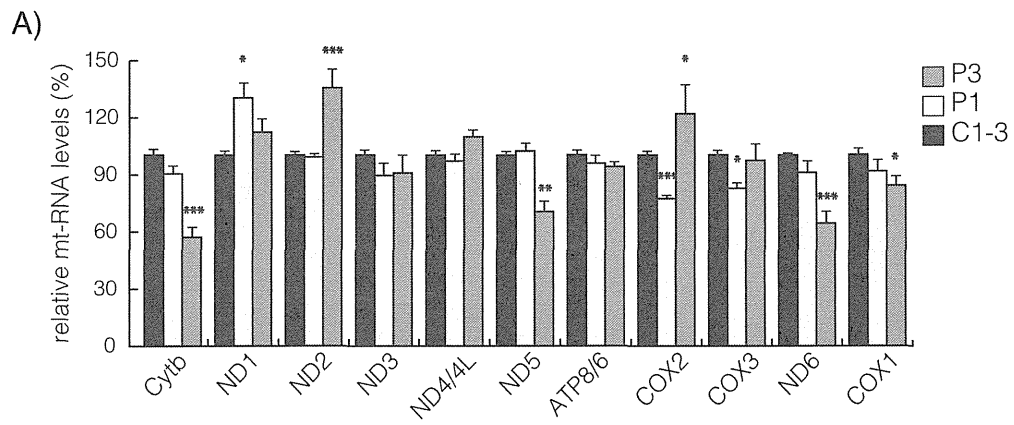


Figure S6: Steady-state levels of the indicated mitochondrial transcripts. Fibroblasts from (A) P1 and P3 or (B) P2 determined by qRT-PCR. All data are represented as mean \pm SEM. (* $p < 0.05$, ** $p < 0.01$, *** $p < 0.001$).

先天代謝異常症におけるトランジションの現状と問題点

高柳 正樹

帝京平成大学地域医療学部看護学科（元千葉県こども病院総合診療科・代謝科）

はじめに

近年トランジションの重要性が声高に言われている理由として、小児期医療の目覚ましい進歩によっても原疾患が治癒に至らず持続していること、合併症が長期に継続し思春期・成人期を迎える患者が増えていることが指摘されている。先天代謝異常症はまさにこの指摘にあるような患者が他の疾患群に比べて多く存在している病態であるといえる。

先天代謝異常症にこのような患者が増えている理由は、表1に示したように、最近の先天代謝異常症の診療をめぐる各種の革新的な診断法や治療法の開発にあると考える。特に治療法の開発は目覚ましく、遺伝子治療などの新治療法がさらに発達すれば、トランジションを要する患者の数はますます増多していくものと考えられる。

日本小児科学会の移行期の患者に関するワーキンググループの「小児期発症疾患を有する患者の移行期医療に関する提言」では、先天代謝異常症は成人診療科に適切な紹介先がなく、小児科で診療を続けることになるのではないかと指摘されている¹⁾。

今回は、一つの小児専門施設における先天代謝異常症の診療部門のトランジションの現状を調査した結果を報告するとともに、今後の先天代謝異常症患者のトランジションのあるべき姿についての夢を述べたい。

目的

千葉県こども病院代謝科を受診した患者のうち、15歳以上の患者の実態を調査することによって、先天代謝異常症患者のトランジションにおける問題

表1 先天代謝異常症：最近何が変わった？

| |
|--|
| めずらしい→考えられていた以上の症例数 |
| 新生児拡大マスキング (MCAD など) |
| The emerging diseases (クレアチニン代謝異常, ビタミン代謝異常) |
| 診断が難しい→診断法の開発 |
| GC/MS |
| MS/MS (タンデムマス) |
| 次世代シーケンサー |
| 治らない→治療法の開発 |
| 酵素補充療法 (MPSI, 2, 6型, Pompe, Fabry, Gaucher) |
| 肝移植, 細胞移植, 幹細胞移植 |
| シャペロン治療 |
| 再生治療 |
| マニアな病気→一般的な病気との関連 |
| 医原性ビオチン・カルニチン欠損症など |

点を明らかにする。

方法

- 1) 千葉県こども病院の診療録から、2014年に代謝科を受診したすべての患者を検索し、その患者を年齢別に分類し分析を加えた。
- 2) これまでに千葉県こども病院を受診したWilson病, ライソゾーム病, リジン尿性タンパク不耐症, メチルマロン酸血症など主な疾患の患者の現在年齢, 現在受診している診療科, 治療法などを調査し、トランジションにおける問題点を検討した。

結果

1. 患者の年齢

2014年に千葉県こども病院代謝科を受診した患者数は438名であった。この患者を5歳ごとの年齢

Special Article : Transition to Adulthood for Children and Adolescents with Metabolic Diseases : Current Status and Issues
Masaki Takayanagi

著者連絡先：高柳正樹（帝京平成大学地域医療学部看護学科）
〒290-0192 千葉県市原市ちはら台西6-19

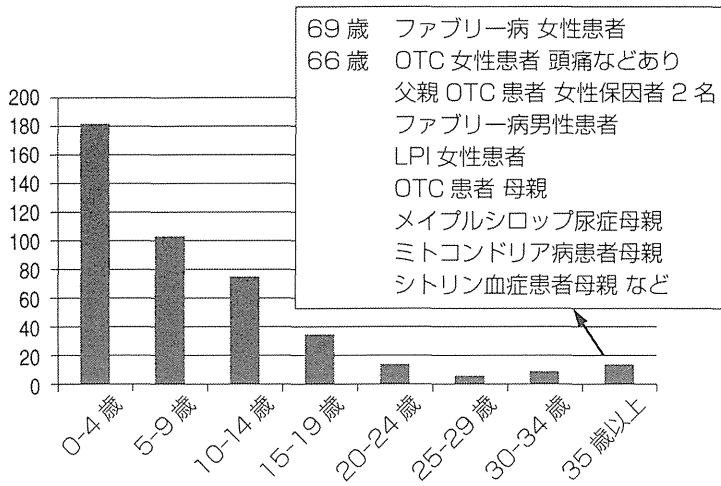


図1 千葉県こども病院代謝科 2014年の受診患者年齢分布

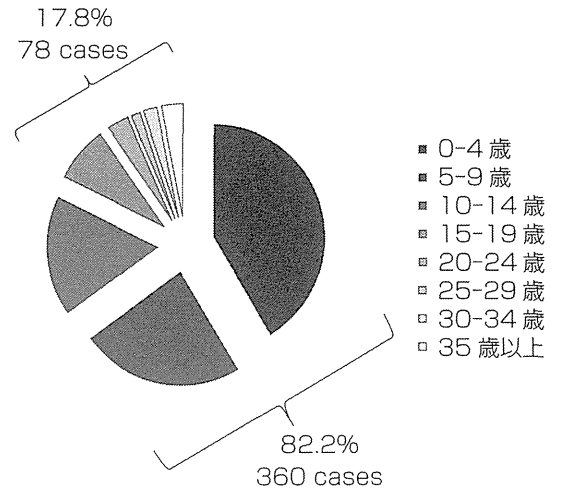


図2 千葉県こども病院代謝科 2014年の受診患者年齢分布 (円グラフ表示)

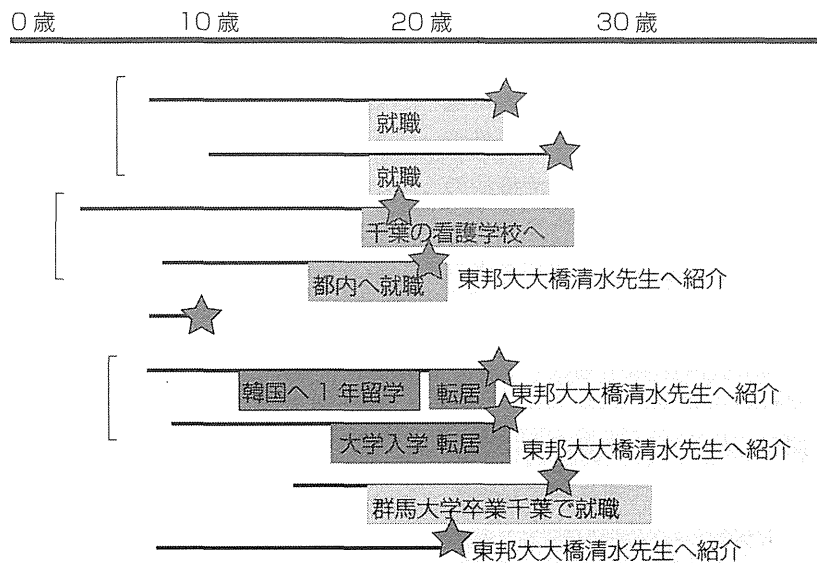


図3 ウィルソン病患者9症例のトランジション

階級に分け図1に表した。さらに、この結果を図2に示した。もちろん、乳幼児に受診者が多いことは当然であるが、15歳以上の患者は78名、17.8%であった。25歳以上の患者は29名、6.6%であり、多くの年長の患者が受診している。最高年齢は69歳のファブリー病の女性患者であった。36歳以上の受診患者の診断名を図1に記載しているが、患者だけでなく、遺伝病である先天代謝異常症の特徴として、患者の母親なども受診している。X染色体関連遺伝病では母親も患者として診療している場合もある。

2. ウィルソン病

最近当院を受診しているウィルソン病は合計9症例であり、そのうち8例が15歳以上であった。図3に、年齢を横軸にトランジションにかかわる事柄を表した。4症例は転居や就職で都内の病院に転院している。

ウィルソン病においては、年長の患者の治療の最重要課題はアドヒアランスとされている。アドヒアランスを良好に保つために、就学・就職問題という時期にいかにして最良な医療機関に転院、トランジションできるかが重要であると考えられた。転院先は小児科医でウィルソン病の専門家がいない病院であ

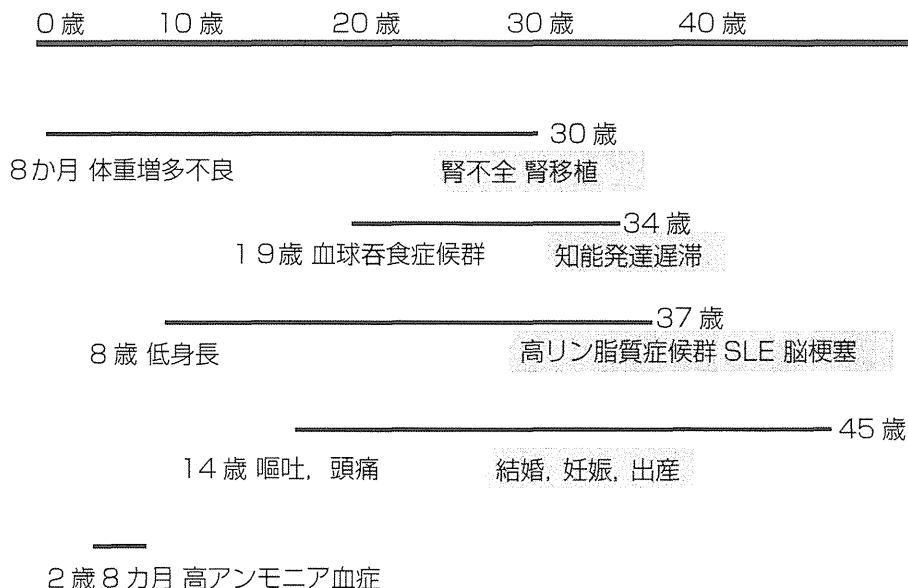


図4 リジン尿性タンパク不対象 (LPI) 4 症例の現在の問題点



図5 ライソゾーム病患者の現在年齢

る。この病院では長くウイルソン病の診療を行っているので、年長の患者も多く診療している実績がある。いわばウイルソン病診断治療部が機能している施設である。先天代謝異常症のトランジションの形として、このような専門診療ユニットを設置し、内科系・小児科系の関連医師が連携して診療を行っていく形も今後考えていくべき方向であると私は考える。

先日ウイルソン病患者を、患者の住居の近くの肝臓専門医の資格を持った内科医師のいる総合病院に紹介したところ、大学病院に紹介してもらいたいとのことであった。ウイルソン病という先天代謝異常症では、昔から内科系の部門の診療経験が多いと考えられる病院でも、適切なトランジション先は得られないのが現状である。

3. リジン尿性タンパク不耐症

図4に、リジン尿性タンパク不耐症の5症例の

経過を示した。リジン尿性タンパク不耐症5症例中4例は30歳以上であった。これら年長者は腎不全、SLE、妊娠出産、知能発達遅滞など広範な臨床的問題を呈しており、成人の内科・外科の関与が必要とされている。

腎移植の患者は腎臓外科の関与が必要であることから、他院の腎臓外科と当院の先天代謝異常の専門家と共同して診療している。SLEの患者は当院受診以前から他院の内科の管理下にあり、共同で診療している形になっているが、同じ病院ではなく緊密な連携で診療ということにはなっていない。45歳の患者は、30年近く小児科医の先天代謝異常専門家が診療している。妊娠・出産時は産科医と情報交換を行い、無事に児を得ることができた。

4. ライソゾーム病

図5に、ライソゾーム病13症例の経過を示した。ライソゾーム病の患者は13症例中10例が15歳以上であった。これら年長者の多くが酵素補充療法を受けている。

ファブリー病はX染色体関連遺伝病であり、一人の患者が発見されると多くの患者が家系内検索で見つかる。このため高齢者を含めて多くの成人患者が発見されている。このような新しく発見される年長患者はトランジションの範疇から離れるが、先天代謝異常症の診療体制を確立するうえで重要な問

題である。このような新しく発見される成人の先天代謝異常症患者の治療体制の確立を契機に、トランジションの環境整備が進む可能性があるかもしれない。具体的には年長のファブリー病の患者さんは循環器内科の診療を受けるように調整している。内科系の医師と顔の見える関係が築ければ、他の代謝異常症に関しても相談がしやすくなるのではないと思われる。

ハーラー、ハンター、アイセル病はすべての症例が重症の中樞神経系障害を呈しており、この意味でトランジションが非常に難しい症例である。

5. メチルマロン酸血症

図6に、メチルマロン酸血症の症例の経過を示した。メチルマロン酸血症は5症例経験したが、新生児発症型の3症例はすべて10歳前後までに死亡している。Late onset typeの2例は、1例が腎不全のため移植を受けている。1例はビタミンB₁₂反応性だが、治療に対するアドヒアランスに問題がある。

メチルマロン酸血症は今後、肝移植、腎移植などの移植医療の適応、効果がよりはっきりしてくれば、長期生存する患者が今以上に増多すると思われる。しかしながら、有機酸代謝異常症は先天代謝異常症の専門家による治療は必須であり、小児科医である先天代謝異常症の専門家が関与し続けなければならない疾患である。トランジションをどのように行えば患者のQOLを保っていけるのかを真剣に考えなければならない。

6. その他

糖原病Ia型の年長児1例は、多発性の肝腫瘍が認められており、腎障害と並び本疾患の年長患者における大きな問題である。この症例は22歳であり通学している大学の関係もあり東京の病院に転院した。転院先の病院には小児科医である先天代謝異常症専門家が勤務している。先天代謝異常症の治療経験が長い病院であるので、院内での内科医との協体制度は成立しており、紹介した成人患者の継続診療には問題がない。一つの病院内で内科系と先天代謝異常症専門医（小児科医が多い）とが協力して、患者さんをきちんと継続して診療していくことのでき

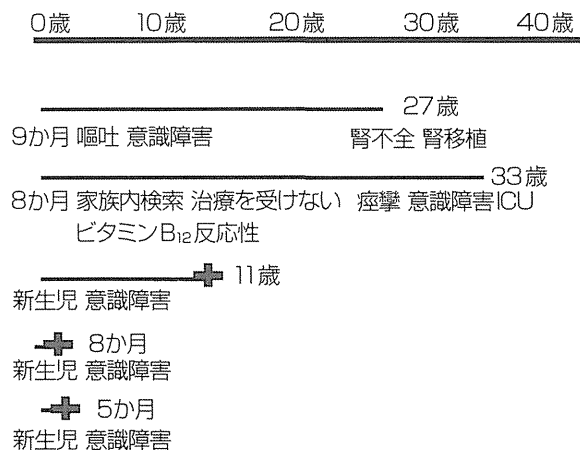


図6 メチルマロン酸血症症例の臨床経過
各症例に発症年齢、その時の主訴、並びに経過中の最大の問題点、死亡年齢、現在年齢を記した。

る羨ましい病院である。

考 察

先天代謝異常症は慢性疾患であるのはもちろんであるが、最近の治療法の進歩や医学管理の充実から、年長の患者、特に15歳を過ぎている患者が急増している。千葉県こども病院の代謝科を受診している患者も15歳以上が17.8%であり、この問題が臨床現場で切実なものになっている。

ことに患者の内科領域の医師への受け渡し（トランジション）は困難である。これは先天代謝異常症の知識を持った内科医がほとんどいないことによるものと思われる。

成人先天性心疾患という分野が、15年以上前から日本においても確立されてきている。千葉県循環器センターでは、小児・成人の循環器小児科医、循環器内科医、循環器外科医さらに専門の看護師も加えて、チーム医療としてこれに対応している^{2,3)}。先天代謝異常症も、これまで診療を行ってきた小児科医中心のチームに内科医に加わってもらい、共同で患者の治療管理にあたるのが必要と考える。

私の経験では、うまくトランジションの患者をお願いできるのは、先天代謝異常症の専門家のいる中規模の総合病院であることが多い。具体的には、大学病院の分院レベルの病院が最適であると思われる。先天代謝異常症について日本全国でこのような病院がいくつあるかは不明であるが、学会が主導してこのような病院における先天代謝異常症専門外来

チームの設立を援助していくことが必須である。

先天代謝異常症は、重篤な中枢神経障害を呈する患者が多いのが一つの特徴である。重篤な中枢神経障害を持った患者の管理は小児科医に経験が多く、さらにこのような成人患者の緊急入院時の入院ベッドの調整が難しいことも指摘されており、成人先天代謝異常症治療管理チームの創設、整備が進んでいくことが望まれる。

千葉県こども病院では増加する在宅医療を確実に実施するために、こども・家族支援センターを設置し、医師だけでなく、看護師、MSW、遺伝カウンセラー、チャイルドライフスペシャリスト、心理士、事務担当を集めて、一つのチームとして機能させている⁴⁾。

トランジションもこのようなチームが必要であり、この在宅医療推進チームの機能をトランジションに使っていくことも一つの方法かと思われる。

結 論

年長の先天代謝異常症の患者を的確に継続的に診

療するためには、現在の小児科医中心の先天代謝異常症診療チームに内科医の参加を求め、共同で治療管理を行っていく必要がある。

さらに、理想的な形としては専門外来を独立して開設して、そこに内科系医師、先天代謝異常専門医などの医師だけでなく、看護師、MSW、遺伝カウンセラー、チャイルドライフスペシャリスト、心理士、事務担当を集めて、一つのチームとして機能するように図ることが望まれる。

文献

- 1) 横谷進, 他. 日本小児科学会移行期の患者に関するワーキンググループ. 小児期発症疾患を有する患者の移行期医療に関する提言. 日本小児科学会雑誌 2014; 118: 98-106
- 2) 丹羽公一郎. 小児科学レビュー 2010; p42-48
- 3) 水野芳子. 日本成人先天性心疾患学会雑誌 2012; 1: 45-48
- 4) 上加世田豊美. コミュニティケア 2009; 11: 55-58

ECHS1 Mutations Cause Combined Respiratory Chain Deficiency Resulting in Leigh Syndrome

Chika Sakai,¹ Seiji Yamaguchi,² Masayuki Sasaki,³ Yusaku Miyamoto,⁴ Yuichi Matsushima,^{1,5*} and Yu-ichi Goto^{1*}

¹ Department of Mental Retardation and Birth Defect Research, National Institute of Neuroscience, National Center of Neurology and Psychiatry, Kodaira, Tokyo, Japan; ² Department of Pediatrics, Shimane University, Izumo, Shimane, Japan; ³ Department of Child Neurology, National Center Hospital, National Center of Neurology and Psychiatry, Kodaira, Tokyo, Japan; ⁴ Department of Pediatrics, St. Marianna University School of Medicine, Kawasaki, Kanagawa, Japan; ⁵ Department of Clinical Chemistry and Laboratory Medicine, Graduate School of Medical Sciences, Kyushu University, Fukuoka, Japan

Communicated by David Rosenblatt

Received 4 September 2014; accepted revised manuscript 5 November 2014.

Published online 13 November 2014 in Wiley Online Library (www.wiley.com/humanmutation). DOI: 10.1002/humu.22730

ABSTRACT: The human *ECHS1* gene encodes the short-chain enoyl coenzyme A hydratase, the enzyme that catalyzes the second step of β -oxidation of fatty acids in the mitochondrial matrix. We report on a boy with *ECHS1* deficiency who was diagnosed with Leigh syndrome at 21 months of age. The patient presented with hypotonia, metabolic acidosis, and developmental delay. A combined respiratory chain deficiency was also observed. Targeted exome sequencing of 776 mitochondria-associated genes encoded by nuclear DNA identified compound heterozygous mutations in *ECHS1*. *ECHS1* protein expression was severely depleted in the patient's skeletal muscle and patient-derived myoblasts; a marked decrease in enzyme activity was also evident in patient-derived myoblasts. Immortalized patient-derived myoblasts that expressed exogenous wild-type *ECHS1* exhibited the recovery of the *ECHS1* activity, indicating that the gene defect was pathogenic. Mitochondrial respiratory complex activity was also mostly restored in these cells, suggesting that there was an unidentified link between deficiency of *ECHS1* and respiratory chain. Here, we describe the patient with *ECHS1* deficiency; these findings will advance our understanding not only the pathology of mitochondrial fatty acid β -oxidation disorders, but also the regulation of mitochondrial metabolism.

Hum Mutat 36:232–239, 2015. © 2014 Wiley Periodicals, Inc.

KEY WORDS: combined respiratory chain deficiency; Leigh syndrome; *ECHS1*; fatty acid β -oxidation disorder

Introduction

Mitochondrial fatty acid β -oxidation provides carbon substrates for gluconeogenesis during the fasting state and contributes electrons to the respiratory chain for energy production. Once a fatty acid is activated to the acyl-coenzyme A (CoA) form and enters the mitochondrial fatty acid β -oxidation pathway, it undergoes the four following enzymatically catalyzed reaction steps during each β -oxidation cycle (Supp. Table S1): (1) dehydrogenation, (2) hydration, (3) a second dehydrogenation step, and finally (4) a thiolytic cleavage that generates one acetyl-CoA or, in certain cases, one propionyl-CoA and an acyl-CoA that is two carbons shorter than the acyl-CoA precursor. Each individual step involves specific enzymes encoded by different genes with different substrate preferences (Supp. Table S1). The first dehydrogenation reaction is catalyzed mainly by four enzymes—short-, medium-, long-, and very long chain acyl-CoA dehydrogenases (SCAD, MCAD, LCAD, and VLCAD)—with substrate optima of C4, C8, C12, and C16 acyl-CoA esters, respectively, still each dehydrogenase can utilize other suboptimal substrates [Ikeda et al., 1983, 1985a, 1985b; Enseauer et al., 2005]. The short-chain enoyl-CoA hydratase (*ECHS1*) catalyzes the next step and has substrate optima of C4 2-trans-enoyl-CoA, also called crotonyl-CoA. Although *ECHS1* also catalyzes hydration of medium chain substrates, longer acyl chains (e.g., C16-intermediates) are hydrated by mitochondrial trifunctional protein (MTP) [Uchida et al., 1992; Kamijo et al., 1993]. MTP consists of an alpha-subunit with long-chain enoyl-CoA hydratase and long-chain 3-hydroxyacyl-CoA dehydrogenase (LCHAD) activities and a beta-subunit with long-chain 3-ketothiolase activity.

Mitochondrial fatty acid β -oxidation disorders generally cause impaired energy production and accumulation of partially oxidized fatty acid metabolites. They are clinically characterized by hypoglycemic seizures, hypotonia, cardiomyopathy, metabolic acidosis, and liver dysfunction [Kompore and Rizzo, 2008]. The most common genetic defect in MTP is LCHAD deficiency [MIM #609016]; deficiency involving reduced activity of all three MTP enzymes [MIM #609015] is reported much less frequently and is often associated with infantile mortality secondary to severe cardiomyopathy [Spiekerkoetter et al., 2004]. Deficiency of SCAD [MIM #201470], which catalyzes the first dehydrogenation reaction and has similar substrate optima with regard to carbon chain as *ECHS1*, have been studied for years, and the range of associated phenotypes includes failure to thrive, metabolic acidosis, ketotic hypoglycemia, developmental delay, seizures, and neuromuscular symptoms such as myopathy and hypotonia [Jethva et al., 2008].

Additional Supporting Information may be found in the online version of this article.

*Correspondence to: Yu-ichi Goto, Department of Mental Retardation and Birth Defect Research, National Institute of Neuroscience, National Center of Neurology and Psychiatry, Kodaira, Tokyo, 187-8502, Japan. E-mail: goto@ncnp.go.jp; Yuichi Matsushima, Department of Clinical Chemistry and Laboratory Medicine, Graduate School of Medical Sciences, Kyushu University, Fukuoka, Fukuoka, 812-8582, Japan. E-mail: matsush5@cclm.med.kyushu-u.ac.jp

Contract grant sponsor(s): Grants-in-Aid for Research on Intractable Diseases (Mitochondrial Disease) from the Ministry of Health, Labor and Welfare of Japan; Research Grant for Nervous and Mental Disorders from the National Center of Neurology and Psychiatry (21A-6, 24-8) and JSPS KAKENHI (25670275).

Here, we describe a patient with ECHS1 deficiency who presented with Leigh syndrome [MIM #256000] accompanied by hypotonia, metabolic acidosis, and developmental delay. Additionally, the patient presented with combined respiratory chain deficiency, which is not commonly described in most clinical reports of mitochondrial fatty acid β -oxidation disorders. Finally, we discuss the pathology of ECHS1 deficiency and possible interactions between mitochondrial fatty acid β -oxidation and the respiratory chain, which are two important pathways in mitochondrial energy metabolism.

Materials and Methods

This study was approved by the ethical committee of National Center of Neurology and Psychiatry. All the samples in this study were taken and used with informed consent from the family.

Whole-mtDNA Genome Sequence Analysis

Long and accurate PCR amplification of mtDNA followed by direct sequencing was performed according to the previous publication with a slight modification [Matsunaga et al., 2005].

Targeted Exome Sequencing

Almost all exonic regions of 776 nuclear genes (Supp. Table S2), in total 7,368 regions, were sequenced using the Target Enrichment System for next-generation sequencing (HaloPlex; Agilent Technologies, Santa Clara, California, USA) and MiSeq platform (Illumina, San Diego, California, USA). Sequence read alignment was performed with a Burrows–Wheeler Aligner (version 0.6.1) to the human reference genome (version hg19). Realignment and recalibration of base quality scores was performed with the Genome Analysis Toolkit (version 1.6.13). Variants were detected and annotated against dbSNP 135 and 1000 Genomes data (February 2012 release) by Quickannotator.

Sanger Sequencing

Sanger sequencing of candidate genes was performed with the BigDye Terminators v1.1 Cycle Sequencing kit (Thermo Fisher Scientific, Waltham, Massachusetts, USA) as per manufacturer's protocol. Details of primers and conditions are available upon request. DNA sequences from the patients were compared against the RefSeq sequence and the sequences of a healthy control or parents those were sequenced in parallel.

Cell Culture

The patient-derived primary myoblasts were established from the biopsy of patient's skeletal muscle and cultured in DMEM/F-12 (Thermo Fisher Scientific) supplemented with 20% (v/v) heat-inactivated fetal bovine serum (FBS, Thermo Fisher Scientific). DLD-1 (human colon carcinoma) cells were provided by Taiho pharmaceutical company (Tokyo, Japan) and cells were cultured in RPMI-1640 (Thermo Fisher Scientific) supplemented with 10% (v/v) heat-inactivated FBS (Thermo Fisher Scientific). All cells were cultured in 5% CO₂ at 37°C.

Preparation of Mitochondrial Fraction

Mitochondrial fractions from patient's skeletal muscle and patient-derived myoblasts were prepared according to the literature with a slight modification [Frezza et al., 2007].

Immunoblotting

Mitochondrial fraction and protein lysates were prepared from patient's skeletal muscle and patient-derived Myoblasts. Thirty micrograms of protein of mitochondrial fraction or 50 micrograms of protein lysate was separated on 4%–12% Bis-Tris gradient gels (Thermo Fisher Scientific) and transferred to polyvinylidene fluoride membranes. Primary antibodies used were against ECHS1 (Sigma-Aldrich, St. Louis, Missouri, USA), complex II 70 kDa subunit (Abcam, Cambridge, England), β -actin (Santa Cruz, Biotechnology, Dallas, Texas, USA), HA (Wako, Tokyo, Japan), and AcGFP (Thermo Fisher Scientific).

Enzyme Assays

Enzyme activities of mitochondrial respiratory complexes I–V and citrate synthase (CS) were measured in mitochondrial fraction prepared from patient's specimens. The assays for complexes I–IV and CS were performed as described previously [Shimazaki et al., 2012]. The assay for complex V was carried out following the method by Morava and his colleagues with modifications [Morava et al., 2006]. The enoyl-CoA hydratase activity was assayed by the hydration of crotonyl-CoA by a slight modification of the procedure described earlier [Steinman and Hill, 1975]. Five micrograms of protein of the mitochondrial fraction prepared from patient-derived myoblasts was added to 0.3 M Tris–HCl, pH 7.4, containing 5 mM EDTA (Ethylenediaminetetraacetic acid). The reaction was started by the addition of 200 μ M crotonyl-CoA and the decrease in absorbance at 280 nm was monitored at 30°C.

Construction of the Immortalized Patient-Derived Myoblasts

The patient-derived myoblasts and control myoblasts were transfected with pEF321-T vector (A kind gift from Dr. Sumio Sugano, University of Tokyo) and the cells were cultured serially for more than ten population doublings until the morphological alteration was observed [Kim et al., 1990].

Expression Vector Preparation and Transfection

For construction of a mammalian expression vector, full-length *ECHS1* (GenBank accession number NM_004092.3) was amplified from a cDNA prepared from control subject using PrimeSTAR GXL DNA polymerase (TaKaRa, Tokyo, Japan). The PCR product was cloned into pEBMulti-Pur (Wako) and the clone was verified by Sanger sequencing. The empty expression vector or an ECHS1 expression vector was transfected into immortalized patient-derived myoblasts using Lipofectamine LTX Reagent (Thermo Fisher Scientific). Each of the two missense variants, c.2T>G; p.M1R and c.5C>T; p.A2V, was independently introduced into the clone by PCR-based site-directed mutagenesis. Each insert with C-terminal HA tag was cloned into pIRES2-AcGFP1 (Clontech Laboratories, Mountain View, California, USA) and the clones were verified by Sanger sequencing. WT and mutant ECHS1 expression vector were transfected into DLD-1 cells using Lipofectamine LTX Reagent (Thermo Fisher Scientific). Twenty-four hours later, the cell lysate was subjected to immunoblotting.

Results

The patient reported here was a boy born to unrelated, healthy parents after a 40-week pregnancy (weight 3,300 g, length 52 cm,

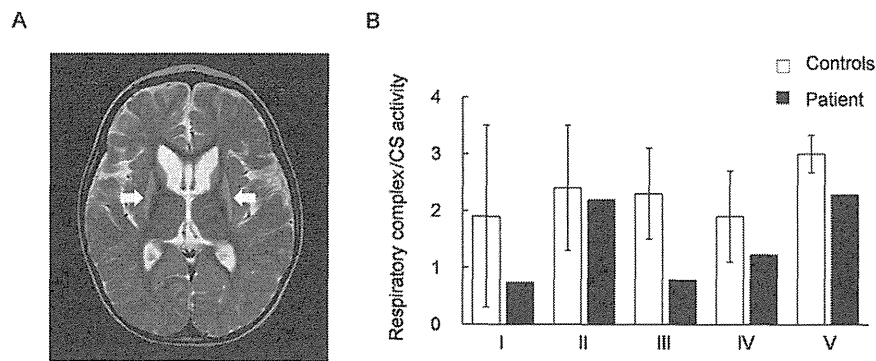


Figure 1. T2-weighted magnetic resonance scan image and enzyme activities of mitochondrial respiratory complexes. **A:** T2-weighted magnetic resonance scan image (MRI) shows bilaterally symmetrical hyperintensities in the putamen (arrows in the image); these are characteristic of Leigh syndrome. **B:** Enzymatic activities of five mitochondrial respiratory complexes (I, II, III, IV, and V) were measured in mitochondrial fractions prepared from the patient's skeletal muscle. Respiratory complexes activities were normalized to citrate synthase activity. Black bars show patient values and white bars show control values. Control values were mean values obtained from five healthy individuals. Patient activity values for complexes I, III, and IV were 39%, 34%, and 64% of the control values, respectively. Error bars represent standard deviations.

Table 1. Urinary Organic Acid Profiling

| | Patient RPA (%) | Controls RPA (%) |
|-----------------------------|--------------------|------------------------|
| TCA cycle intermediates | | |
| α -Ketoglutarate | 4.52 | 3.00–102.90 |
| Aconitate | 20.37 | 15.10–86.10 |
| Isocitrate | 8.98 | 8.30–29.00 |
| Other metabolites | | |
| Lactate | 11.83 ^a | <4.70 |
| Pyruvate | 3.18 | <24.10 |
| 3-Hydroxyisobutyric acid | 1.95 | <9.00 |
| Methylcitric acid | 0.14 ^a | Less than trace amount |
| p-Hydroxy-phenyllactic acid | 40.05 ^a | <7.00 |
| Glyoxylate | 37.71 ^a | <6.10 |

^aValues outside the normal range.

RPA(%), relative peak area to the area of internal standard (heptadecanoic acid, HDA).

occipitofrontal circumference (OFC) 34.5 cm). Auditory screening test at 2 months of age revealed hearing impairment, and he began to use a hearing aid at 6 months of age. Psychomotor developmental delay was noted at 5 months of age; he could not sit alone, or speak a meaningful word as of 4 years of age. Nystagmus was noted at 10 months of age. Muscle hypotonia, spasticity, and athetotic trunk movement became prominent after 1 year of age. His plasma (20.2 mg/dl) and a cerebrospinal fluid lactate were elevated (25.3 mg/dl, control below 15 mg/dl). Urinary organic acid profiling reveals significantly elevated excretion of glyoxylate (Table 1). Analysis of blood acylcarnitines showed no abnormalities. Brain magnetic resonance scan image showed bilateral T2 hyperintensity of the putamen, typical for Leigh syndrome (Fig. 1A). Because Leigh syndrome is generally caused by defects in the mitochondrial respiratory chain or the pyruvate dehydrogenase complex, we performed a muscle biopsy to measure enzyme activities of mitochondrial respiratory complexes in the patient. Mitochondrial fractions prepared from patient or control specimens were used for all activity measurements. Activity of each respiratory complex was normalized relative to CS activity; normalized values for complexes I, III, and IV activity were decreased to 39%, 34%, and 64% of control values, respectively (Fig. 1B). Moreover, we performed blue native PAGE (BN-PAGE) to examine if the assembly of respiratory complexes were altered in the patient. As a result, there were no clear difference between the patient and the control (Supp. Fig. S1).

Mitochondrial respiratory chain defects can be due to pathogenic mutations in mitochondrial DNA (mtDNA) or nuclear DNA (nDNA) coding for mitochondrial components. Initially, long and accurate PCR amplification of mtDNA followed by direct sequencing was performed and no mutations known to be associated with Leigh syndrome were identified, but previously reported polymorphisms were found (Supp. Table S3). Therefore, to identify the responsible mutations in nDNA, targeted exome sequencing was performed. Coverage was at least 10 \times for 86.2% of the target regions, and 30 \times or more for 73.4%. In all, 5,640 potential variants were identified; these included 811 splice-site or nonsynonymous variants. Among those 811 variants, 562 were on the mismatching reads that contained multiple apparent mismatches to the reference DNA sequence. Of the remaining 249 variants, nine that were on target regions with less than 10 \times coverage were eliminated because data reliability was low. Filtering against dbSNP 135 and 1000 Genomes data, this number was reduced to 13 including compound heterozygous variants in the *ECHS1* [MIM #602292] and 11 heterozygous variants in 11 separate genes (Supp. Table S4). Those variants have been submitted to dbSNP (<http://www.ncbi.nlm.nih.gov/SNP/>). Because most mitochondrial diseases caused by known nDNA mutations are inherited in an autosomal recessive manner, we focused on the compound heterozygous variants in *ECHS1*—c.2T>G; p.M1R and c.5C>T; p.A2V—as primary candidates.

To confirm the targeted exome sequencing results, we performed Sanger sequencing of genomic *ECHS1* DNA and *ECHS1* cDNA from the patient and his parents. We identified both variants, c.2T>G and c.5C>T, and the respective normal alleles in genomic DNA and cDNA from the patient (Fig. 2A and B) and no other *ECHS1* variants were detected except for common SNPs in the open reading frame. Analysis of genomic DNA from the patient's parents showed that patient's father was heterozygous for only one variant, c.2T>G, and the patient's mother for only the other variant, c.5C>T (Fig. 2A). These results indicated that the patient inherited each variant separately and that both mutant alleles were expressed in the patient (Fig. 2B). Each variant was nonsynonymous and in the region encoding the mitochondrial transit peptide (1–27 amino acids) of *ECHS1* [Hochstrasser et al., 1992]; moreover, c.2T>G; p.M1R was a start codon variant (Fig. 2C).

Next, immunoblotting with primary antibodies against *ECHS1* was performed to assess protein expression. Mitochondrial

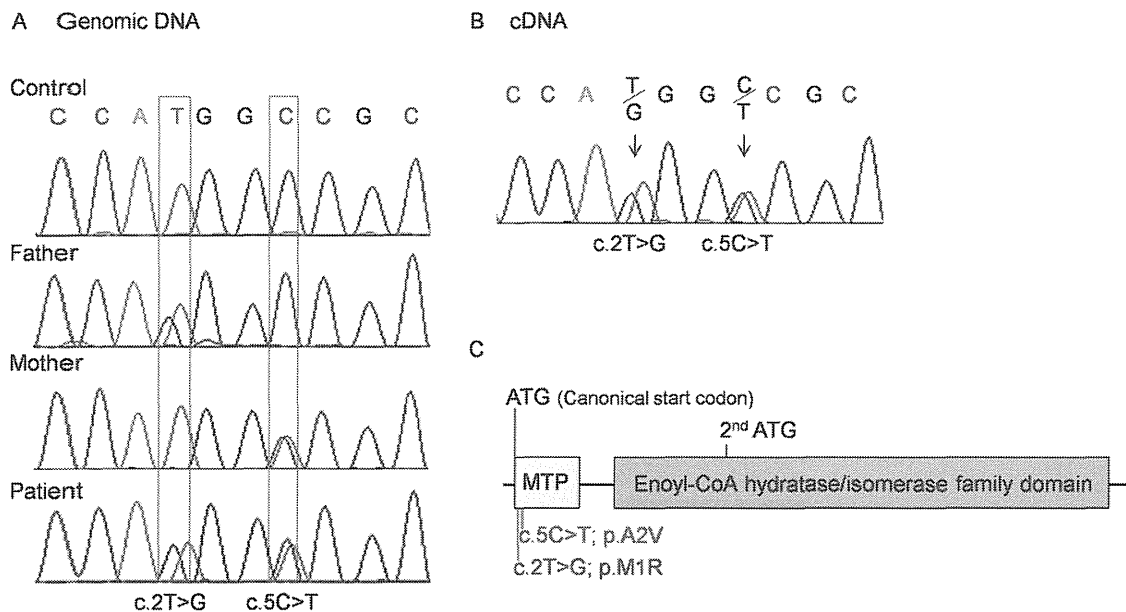


Figure 2. *ECHS1* Sanger sequencing analysis and *ECHS1* functional domains. **A:** Sequence chromatograms from part of exon 1 of *ECHS1* were generated by Sanger sequencing of genomic DNA. Each parent had one wild-type allele; the patient's father also harbored a c.2T>G variant, and the patient's mother a c.5C>T variant. The patient inherited each variant allele and was a compound heterozygote. **B:** Sequence chromatograms from part of *ECHS1* exon 1 obtained by Sanger sequencing of cDNA prepared from patient mRNA. The same variants seen in genomic DNA were observed in the cDNA. **C:** A schematic diagram of the functional domains in *ECHS1* and the locations of the mutations. MTP, mitochondrial transit peptide.

fractions prepared from patient and control skeletal muscle were used; whole-cell lysates or mitochondrial fractions prepared from patient-derived or control myoblasts were also used. All experiments using these specimens showed that the expression level of *ECHS1* protein of the patient was too low to detect by immunoblotting even though the expression level of *SDHA* was almost the same as controls (Fig. 3A–C). These findings indicated that c.2T>G; p.M1R and c.5C>T; p.A2V mutations caused a remarkable reduction in *ECHS1* protein expression. Notably, patient-derived and control myoblasts were similar with regard to *ECHS1* mRNA expression (Fig. 3D), indicating that the mutations apparently affected *ECHS1* protein expression directly. Next, we measured *ECHS1* enzyme activity in mitochondrial fractions prepared from patient-derived and control myoblasts. *ECHS1* activity was normalized to CS activity, and activity in patient-derived myoblasts was 13% of that in control myoblasts (Fig. 3E). Therefore, the mutations caused a severe depletion of *ECHS1* protein expression thereby decreasing *ECHS1* enzyme activity.

To examine the stability of each mutated protein, we constructed three pIRES2-AcGFP1 expression plasmids, each expressed a different HA-tagged protein: wild-type, M1R-mutant, or A2V-mutant *ECHS1*. The expression of AcGFP was used as a transfection control. After the transfection into DLD-1 cells, immunoblotting of whole-cell lysate with anti-HA and GFP antibodies showed markedly higher expression of wild-type *ECHS1* than of either mutant protein; all *ECHS1* expression was normalized to AcGFP expression (Fig. 4, Supp. Fig. S2). This result indicated that *ECHS1* protein expression was significantly reduced in the patient because of each mutation.

To confirm that the patient had *ECHS1* deficiency, we performed a cellular complementation experiment. Patient-derived myoblasts had to be immortalized for these experiments because nonimmortalized cells exhibited poor growth and finite proliferation. The patient-derived myoblasts and control myoblasts were transfected with pEF321-T vector (a kind gift from Dr. Sumio Sugano, Uni-

versity of Tokyo). We then ascertained that *ECHS1* protein expression and activity were lower in immortalized patient-derived myoblasts than in controls (Fig. 5A and B). We then transduced an empty expression vector, pEBMulti-Pur (Wako), or a pEBMulti-Pur construct containing a full-length, wild-type *ECHS1* cDNA into the immortalized patient-derived myoblasts; cells with the vector only or the *ECHS1*-expression construct are hereafter called vector-only and rescued myoblasts, respectively. *ECHS1* protein expression level and enzyme activity were analyzed in mitochondrial fractions prepared from rescued myoblasts. Relative expression level of *ECHS1* in rescued myoblasts was 11 times higher than that in vector-only myoblasts (Fig. 5A), and *ECHS1* activity normalized to CS activity in rescued myoblasts was 49 times higher than that in vector-only myoblasts (Fig. 5B). From these cellular complementation experiments, we concluded the patient had *ECHS1* deficiency.

Since the patient showed the combined mitochondrial respiratory chain deficiency in the skeletal muscle as mentioned above, we used a cellular complementation experiment to determine whether wild-type *ECHS1* rescued the respiratory chain defect in patient-derived myoblasts. First, we measured enzyme activities of each mitochondrial respiratory complex in mitochondrial fractions prepared from immortalized patient-derived myoblasts. CS activity normalized values for complexes I, IV, and V activity in immortalized patient-derived myoblasts were decreased to 17%, 39%, and 43% of the mean values of immortalized control myoblasts (Fig. 5C). Then, we measured enzyme activity in mitochondrial fractions prepared from rescued myoblasts and found that each activity of complexes I, IV, and V was mostly restored relative to that in vector-only myoblasts. In rescued myoblasts, CS activity normalized values of complexes I, IV, and V were 3.5, 1.3, and 2.2 times higher than those in vector-only myoblasts (Fig. 5C). Mitochondrial respiratory complex activity was mostly restored in rescued myoblasts, suggesting that there was an unidentified link between deficiency of *ECHS1* and respiratory chain.

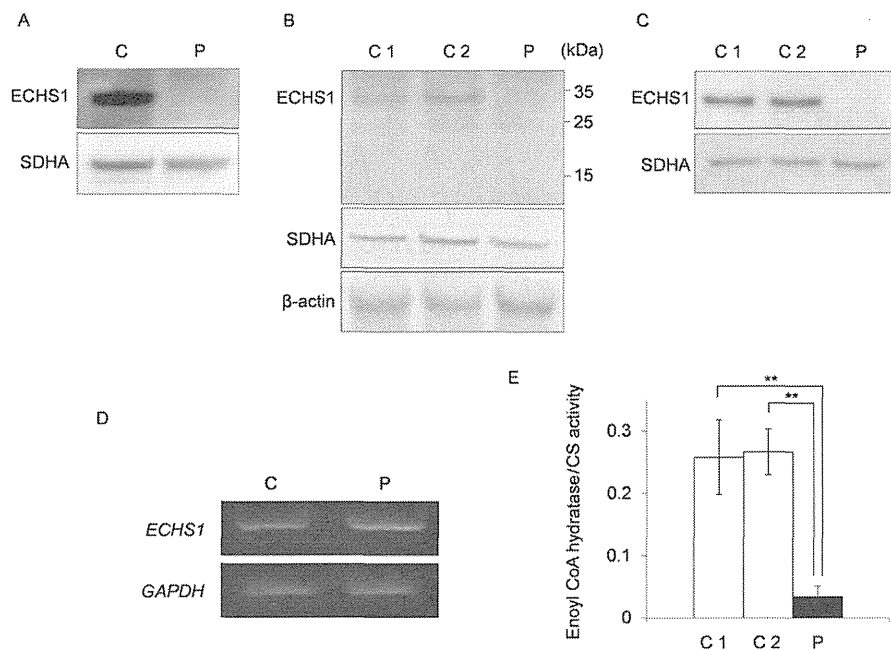


Figure 3. ECHS1 expression and enzyme activity. ECHS1 expression was analyzed by immunoblotting. C1/2, control; P, patient. Mitochondrial fraction prepared from patient's skeletal muscle (A) or whole-cell lysate (B) and mitochondrial fraction (C) prepared from the patient-derived myoblasts were analyzed via immunoblotting. All findings indicated that ECHS1 levels in patient samples were too low to detect by immunoblotting. D: RT-PCR was used to assess *ECHS1* mRNA levels in the patient. Notably, patient-derived myoblasts and control myoblasts did not differ with regard to *ECHS1* mRNA level. E: Mitochondrial fractions prepared from patient-derived myoblasts were used to estimate ECHS1 enzyme activity in the patient. All ECHS1 activity measurements were normalized to CS activity; ECHS1 activity in patient-derived samples was 13% of that in control samples. The experiments were performed in triplicate. Error bars represent standard deviations. (** $P < 0.005$ Student's *t*-test).

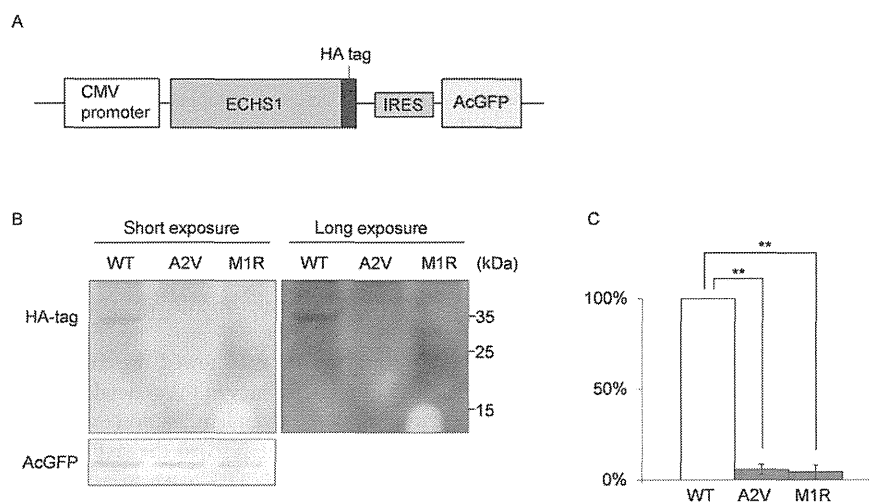


Figure 4. Exogenous expression of mutant ECHS1 protein in cancer cells. A: Schematic diagram of the pIRES mammalian expression vector. B: Representative image of an immunoblotting containing AcGFP, an internal control, and each HA-tagged ECHS1 protein; all proteins were isolated from DLD-1 cells that transiently overexpressed wild-type, A2V, or M1R HA-tagged ECHS1 from pIRES. The images obtained by short exposure (left) and long exposure (right). C: Overexpressed HA-tagged ECHS1 protein levels. Both mutant ECHS1 proteins showed dramatically decreased expression compared to wild-type ECHS1 protein, when ECHS1 was normalized relative to the internal control. Each experiment was performed in triplicate. Error bars represent standard deviations (** $P < 0.005$ Student's *t*-test).

Discussion

Here, we described a patient harboring compound heterozygous mutations in *ECHS1*. Immunoblotting analysis revealed that ECHS1 protein was undetectable in patient-derived myoblasts; moreover, these cells showed significantly lower ECHS1 enzyme activity than

controls. Exogenous expression of two recombinant mutant proteins in DLD-1 cells showed c.2T>G; p.M1R and c.5C>T; p.A2V mutations affected ECHS1 protein expression. Cellular complementation experiment verified the patient had ECHS1 deficiency.

The c.2T>G; p.M1R mutation affected the start codon and therefore was predicted to impair the protein synthesis from canonical

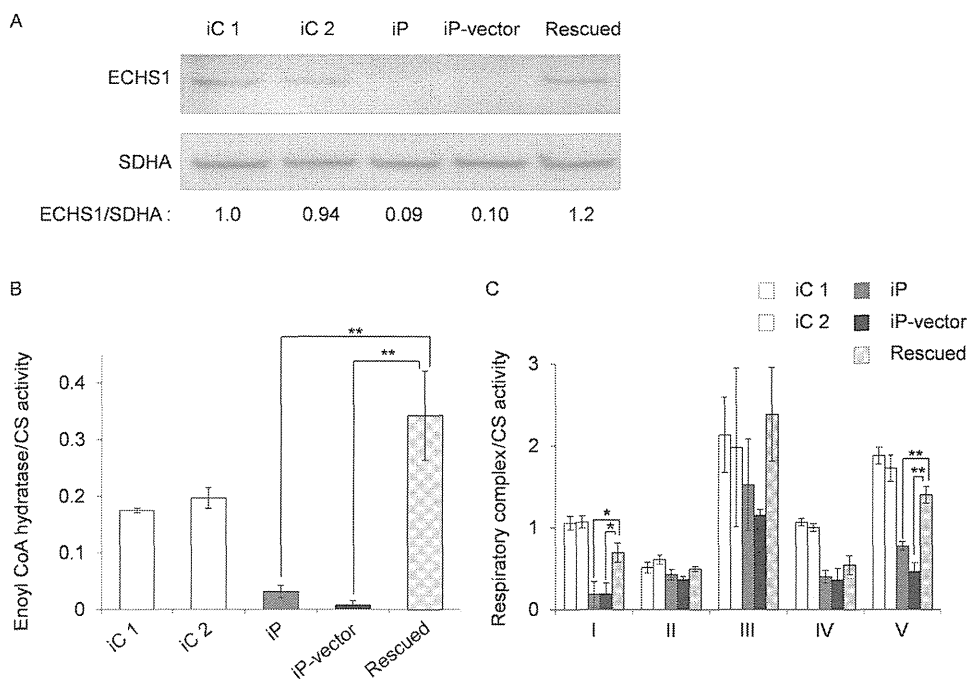


Figure 5. ECHS1 protein expression and enzyme activity in rescued myoblasts. An empty vector or a construct encoding wild-type ECHS1 was introduced into immortalized patient-derived myoblasts. iC1/2, immortalized control myoblasts; iP, immortalized patient-derived myoblasts; iP-vector, immortalized patient-derived myoblasts transfected with empty vector; Rescued, immortalized patient-derived myoblasts stably expressing wild-type ECHS1. **A:** ECHS1 levels were assessed on immunoblotting using mitochondrial fractions prepared from rescued myoblasts. ECHS1 level in “rescued” is 11 times higher than that in “iP-vector”. **B:** Mitochondrial fractions prepared from rescued myoblasts were also used to measure ECHS1 enzyme activity. ECHS1 activity normalized to CS activity in “rescued” was 49 times higher than that in “iP-vector.” Each experiment was performed in triplicate. Error bars represent standard deviations (** $P < 0.005$ Student’s *t*-test). **C:** Mitochondrial fractions prepared from rescued myoblasts were used to measure enzyme activities of mitochondrial respiratory complexes. Activity values were normalized to CS activity. Activities of complexes I, IV, and V were mostly restored from “iP” and “iP-vector.” In “rescued,” the enzyme activities of complexes I, IV, and V were 3.5, 1.3, and 2.2 times higher, respectively, than the “iP-vector.” Each experiment was performed in triplicate. Error bars represent standard deviations (** $P < 0.005$, * $P < 0.05$ Student’s *t*-test).

initiation site. In the reference *ECHS1* sequence, the next in-frame start codon is located in amino acids 97 (Fig. 2C). Even if translation could occur from this second start codon, the resulting product would lack the whole transit peptide and part of the enoyl-CoA hydratase/isomerase family domain (Fig. 2C). The c.5C>T; p.A2V mutation was located in the mitochondrial transit peptide and the mutation may affect the mitochondrial translocation of ECHS1. Surprisingly, the MitoProt-predicted mitochondrial targeting scores for the wild-type and A2V-mutant proteins were 0.988 and 0.991, respectively [MitoProt II; <http://ihg.gsf.de/ihg/mitoprot.html>; Claros and Vincens, 1996] and not markedly different from each other. Nevertheless, mislocalized mutant protein may have been degraded outside of the mitochondria. Consistent with this speculation was the finding that immunoblotting of lysate from patient-derived myoblasts (Fig. 3B) or from transfected cells that overexpressed the recombinant p.A2V-mutant ECHS1 (Fig. 4B, Supp. Fig. S2) did not show upper shifted ECHS1 bands that indicated ECHS1 with the transit peptide. Another possible explanation is that the mutation affected the translation efficiency because it was very close to the canonical start codon. It can change secondary structure of ECHS1 mRNA or alter the recognition by the translation initiation factors. As stated above, even if there was a translation product from the second in-frame start codon, that product would probably not function.

This patient presented with symptoms that are indicative of fatty acid oxidation disorders (e.g., hypotonia and metabolic acidosis), but he also presented with neurologic manifestations, in-

cluding developmental delay and Leigh syndrome, that are not normally associated with fatty acid β -oxidation disorders. Interestingly, developmental delay is also found in cases of SCAD deficiency [Jethva et al., 2008]. In the absence of SCAD, the byproducts of butyryl-CoA—including butyrylcarnitine, butyrylglycine, ethylmalonic acid (EMA), and methylsuccinic acid—accumulate in blood, urine, and cells. These byproducts may cause the neurological pathology associated with SCAD deficiency [Jethva et al., 2008]. EMA significantly inhibits creatine kinase activity in the cerebral cortex of Wistar rats but does not affect levels in skeletal or heart muscle [Corydon et al., 1996]. Elevated levels of butyric acid modulated gene expression because excess butyric acid can enhance histone deacetylase activity [Chen et al., 2003]. Moreover, the highly volatile nature of butyric acid as a free acid may also add to its neurotoxic effects [Jethva et al., 2008].

On the other hand, it is very rare for fatty acid β -oxidation disorders causing Leigh syndrome. Therefore, the most noteworthy manifestation in this patient was Leigh syndrome. Leigh syndrome is a neuropathological entity characterized by symmetrical necrotic lesions along the brainstem, diencephalon, and basal ganglion [Leigh, 1951]. It is caused by abnormalities of mitochondrial energy generation and exhibits considerable clinical and genetic heterogeneity [Chol et al., 2003]. Commonly, defects in the mitochondrial respiratory chain or the pyruvate dehydrogenase complex are responsible for this disease. This patient’s skeletal muscle samples exhibited a combined respiratory chain deficiency, and this deficiency may be the reason that he presented with Leigh syndrome. Although it

remained unclear what caused the respiratory chain defect, cellular complementation experiments showed almost complete restoration, indicating there was an unidentified link between ECHS1 and respiratory chain. One of the possible causes of respiratory chain defect is the secondary effect of accumulation of toxic metabolites. For example, an elevated urine glyoxylate was observed in this patient. Although the mechanism of this abnormal accumulation is not clear at the moment, it was shown that glyoxylate inhibited oxidative phosphorylation or pyruvate dehydrogenase complex by *in vitro* systems [Whitehouse et al., 1974; Lucas and Pons, 1975]. Therefore, we speculate that in our patient, ECHS1 deficiency induced metabolism abnormality including glyoxylate accumulation, and glyoxylate played a role in decreased enzyme activities of respiratory chain complexes. Interestingly, a recent paper describing patients with Leigh syndrome and ECHS1 deficiency showed decreased activity of pyruvate dehydrogenase complex in fibroblasts [Peters et al., 2014], (Supp. Table S5). BN-PAGE showed the assembly of respiratory complex components in the patient was not clearly different from the control (Supp. Fig. S1). This result suggests that the respiratory chain defect in the patient is more likely because of the secondary effect of accumulation of toxic metabolites. On the other hand, many findings indicate interplays between mitochondrial fatty acid β -oxidation and the respiratory chain. For example, Enns et al. [2000] mentioned the possibility of the physical association between these two energy-generating pathways from overlapping clinical phenotypes in genetic deficiency states. More recently, Wang and his colleagues actually showed physical association between mitochondrial fatty acid β -oxidation enzymes and respiratory chain complexes (Wang et al., 2010). Similarly, Narayan et al. demonstrated interactions between short-chain 3-hydroxyacyl-CoA dehydrogenase (SCHAD) and several components of the respiratory chain complexes including the catalytic subunits of complexes I, II, III, and IV via pull-down assays involving several mouse tissues. Considering the role of SCHAD as a NADH-generating enzyme, this interaction was suggested to demonstrate the logical physical association with the regeneration of NAD through the respiratory chain [Narayan et al., 2012]. Still more recently, mitochondrial protein acetylation was found to be driven by acetyl-CoA produced from mitochondrial fatty acid β -oxidation [Pougovkina et al., 2014]. Because the activities of respiratory chain enzymes are regulated by protein acetylation [Zhang et al., 2012], this finding indicated that β -oxidation regulates the mitochondrial respiratory chain. Remarkably, acyl-CoA dehydrogenase 9 (ACAD9), which participates in the oxidation of unsaturated fatty acid, was recently identified as a factor involved in complex I biogenesis [Haack et al., 2010; Heide et al., 2012]. Cellular complementation experiments that involve overexpression of wild-type ACAD9 in patient-derived fibroblast cell lines showed restoration of complex I assembly and activity [Haack et al., 2010]. Accumulating evidence indicates that there are complex regulatory interactions between mitochondrial fatty acid β -oxidation and the respiratory chain.

ECHS1 has been shown to interact with several molecules outside the mitochondrial fatty acid β -oxidation pathway [Chang et al., 2013; Xiao et al., 2013] and the loss of this interaction can affect respiratory chain function in a patient. Further functional analysis of ECHS1 will advance our understanding of the complex regulation of mitochondrial metabolism.

Acknowledgments

We acknowledge the technical support of Dr. Ichizo Nishino, Dr. Ikuya Nonaka, Dr. Chikako Waga, Takao Uchiumi, Yoshie Sawano, and Michiyo

Nakamura. We also thank Dr. Sumio Sugano (the University of Tokyo) for providing the pEF321-T plasmid.

Disclosure statement: The authors have no conflict of interest to declare.

References

- Chang Y, Wang SX, Wang YB, Zhou J, Li WH, Wang N, Fang DF, Li HY, Li AL, Zhang XM, Zhang WN. 2013. ECHS1 interacts with STAT3 and negatively regulates STAT3 signaling. *FEBS Lett* 587:607–613.
- Chen JS, Faller DV, Spanjaard RA. 2003. Short-chain fatty acid inhibitors of histone deacetylases: promising anticancer therapeutics? *Curr Cancer Drug Targets* 3:219–236.
- Choi M, Lebon S, Bénit P, Chretien D, de Lonlay P, Goldenberg A, Odent S, Hertz-Pannier L, Vincent-Delorme C, Cormier-Daire V, Rustin P, Rötig A, et al. 2003. The mitochondrial DNA G13513A MELAS mutation in the NADH dehydrogenase 5 gene is a frequent cause of Leigh-like syndrome with isolated complex I deficiency. *J Med Genet* 40:188–191.
- Claros MG, Vincens P. 1996. Computational method to predict mitochondrially imported proteins and their targeting sequences. *Eur J Biochem* 241:779–786.
- Corydon MJ, Gregersen N, Lehnert W, Ribes A, Rinaldo P, Kmoch S, Christensen E, Kristensen TJ, Andresen BS, Bross P, Winter V, Martinez G, et al. 1996. Ethylmalonic aciduria is associated with an amino acid variant of short chain acyl-coenzyme A dehydrogenase. *Pediatr Res* 39:1059–1066.
- Enns GM, Bennett MJ, Hoppel CL, Goodman SI, Weisiger K, Ohnstad C, Golabi M, Packman S. 2000. Mitochondrial respiratory chain complex I deficiency with clinical and biochemical features of long-chain 3-hydroxyacyl-coenzyme A dehydrogenase deficiency. *J Pediatr* 136:251–254.
- Ensenauer R, He M, Willard JM, Goetzman ES, Corydon TJ, Vandahl BB, Mohsen A-W, Isaya G, Vockley J. 2005. Human acyl-CoA dehydrogenase-9 plays a novel role in the mitochondrial beta-oxidation of unsaturated fatty acids. *J Biol Chem* 280:32309–32016.
- Frezza C, Cipolat S, Scorrano L. 2007. Organelle isolation: functional mitochondria from mouse liver, muscle and cultured fibroblasts. *Nat Protoc* 2:287–295.
- Haack TB, Danhauser K, Haberberger B, Hoser J, Strecker V, Boehm D, Uziel G, Lamantea E, Invernizzi F, Poulton J, Rolinski B, Iuso A, et al. 2010. Exome sequencing identifies ACAD9 mutations as a cause of complex I deficiency. *Nat Genet* 42:1131–1134.
- Heide H, Bleier L, Steger M, Ackermann J, Dröse S, Schwamb B, Zörnig M, Reichert AS, Koch I, Wittig I, Brandt U. 2012. Complexome profiling identifies TMEM126B as a component of the mitochondrial complex I assembly complex. *Cell Metab* 6:538–549.
- Hochstrasser DF, Frutiger S, Paquet N, Bairoch A, Ravier F, Pasquali C, Sanchez JC, Tissot JD, Bjellqvist B, Vargas R, Ron DA, Graham JH. 1992. Human liver protein map: a reference database established by microsequencing and gel comparison. *Electrophoresis* 13:992–1001.
- Ikeda Y, Dabrowski C, Tanaka K. 1983. Separation and properties of five distinct acyl-CoA dehydrogenases from rat liver mitochondria. *J Biol Chem* 258:1066–1076.
- Ikeda Y, Hine DG, Okamura-Ikeda K, Tanaka K. 1985a. Mechanism of action of short-chain, medium chain and long-chain acyl-CoA dehydrogenases: direct evidence for carbanion formation as an intermediate step using enzyme-catalyzed C-2 proton/deuteron exchange in the absence of C-3 exchange. *J Biol Chem* 260:1326–1337.
- Ikeda Y, Okamura-Ikeda K, Tanaka K. 1985b. Spectroscopic analysis of the interaction of rat liver short chain, medium chain and long chain acyl-CoA dehydrogenases with acyl-CoA substrates. *Biochemistry* 24:7192–7199.
- Jethva R, Bennett MJ, Vockley J. 2008. Short-chain acyl-coenzyme A dehydrogenase deficiency. *Mol Genet Metab* 95:195–200.
- Kamijo T, Aoyama T, Miyazaki J, Hashimoto T. 1993. Molecular cloning of the cDNAs for the subunits of rat mitochondrial fatty acid beta-oxidation multienzyme complex. Structural and functional relationships to other mitochondrial and peroxisomal beta-oxidation enzymes. *J Biol Chem* 268:26452–26460.
- Kim DW, Uetsuki T, Kaziro Y, Yamaguchi N, Sugano S. 1990. Use of the human elongation factor 1 alpha promoter as a versatile and efficient expression system. *Gene* 91:217–223.
- Kompare M, Rizzo WB. 2008. Mitochondrial fatty-acid oxidation disorders. *Semin Pediatr Neurol* 15:140–149.
- Leigh D. 1951. Subacute necrotizing encephalomyelopathy in an infant. *J Neurol Neurosurg Psychiatr* 14:216–221.
- Lucas M, Pons AM. 1975. Influence of glyoxylic acid on properties of isolated mitochondria. *Biochimie* 57:637–645.
- Matsunaga T, Kumanomido H, Shiroma M, Goto Y, Usami S. 2005. Audiological features and mitochondrial DNA sequence in a large family carrying mitochondrial A1555G mutation without use of aminoglycoside. *Ann Otol Rhinol Laryngol* 114:153–160.

- Morava E, Rodenburg RJ, Hol F, de Vries M, Janssen A, van den Heuvel L, Nijtmans L, Smeitink J. 2006. Clinical and biochemical characteristics in patients with a high mutant load of the mitochondrial T8993G/C mutations. *Am J Med Genet A* 140:863–868.
- Narayan, SB, Master SR, Sirec AN, Bierl C, Stanley PE, Li C, Stanley CA, Bennett MJ. 2012. Short-chain 3-hydroxyacyl-coenzyme A dehydrogenase associates with a protein super-complex integrating multiple metabolic pathways. *PLoS One* 7: e35048.
- Peters H, Buck N, Wanders R, Ruiten J, Waterham H, Koster J, Yapliito-Lee J, Ferdinandusse S, Pitt J. 2014. ECHS1 mutations in Leigh disease: a new inborn error of metabolism affecting valine metabolism. *Brain* 137: 2903–2908.
- Pougovkina O, Te Brinke H, Ofman R, van Cruchten AG, Kulik W, Wanders RJ, Houten SM, de Boer VC. 2014. Mitochondrial protein acetylation is driven by acetyl-CoA from fatty acid oxidation. *Hum Mol Genet* 23:3513–3522.
- Shimazaki H, Takiyama Y, Ishiura H, Sakai C, Matsushima Y, Hatakeyama H, Honda J, Sakoe K, Naoi T, Namekawa M, Fukuda Y, Takahashi Y, et al. 2012. A homozygous mutation of C12orf65 causes spastic paraplegia with optic atrophy and neuropathy (SPG55). *J Med Genet* 49:777–784.
- Spiekerkoetter U, Khuchua Z, Yue Z, Bennett MJ, Strauss AW. 2004. General mitochondrial trifunctional protein (TFP) deficiency as a result of either alpha- or beta-subunit mutations exhibits similar phenotypes because mutations in either subunit alter TFP complex expression and subunit turnover. *Pediatr Res* 55:190–196.
- Steinman HM, Hill RL. 1975. Bovine liver crotonase (enoyl coenzyme A hydratase). *Methods Enzymol* 35:136–151.
- Uchida Y, Izai K, Orii T, Hashimoto T. 1992. Novel fatty acid beta-oxidation enzymes in rat liver mitochondria. II. Purification and properties of enoyl-coenzyme A (CoA) hydratase/3-hydroxyacyl-CoA dehydrogenase/3-ketoacyl-CoA thiolase trifunctional protein. *J Biol Chem* 267:1034–1041.
- Wang Y, Mohsen AW, Mihalik SJ, Goetzman ES, Vockley J. 2010. Evidence for physical association of mitochondrial fatty acid oxidation and oxidative phosphorylation complexes. *J Biol Chem* 285:29834–29841.
- Whitehouse S, Cooper RH, Randle PJ. 1974. Mechanism of activation of pyruvate dehydrogenase by dichloroacetate and other halogenated carboxylic acids. *Biochem J* 141:761–774.
- Xiao CX, Yang XN, Huang QW, Zhang YQ, Lin BY, Liu JJ, Liu YP, Jazag A, Guleng B, Ren JL. 2013. ECHS1 acts as a novel HBsAg-binding protein enhancing apoptosis through the mitochondrial pathway in HepG2 cells. *Cancer Lett* 330:67–73.
- Zhang J, Lin A, Powers J, Lam MP, Lotz C, Liem D, Lau E, Wang D, Deng N, Korge P, Zong, NC, Cai H, et al. 2012. Perspectives on: SGP symposium on mitochondrial physiology and medicine: mitochondrial proteome design: from molecular identity to pathophysiological regulation. *J Gen Physiol* 139:395–406.

グリコーゲン代謝：筋肉から脳へ

杉江秀夫

要旨 筆者らは主にグリコーゲンの代謝障害に起因する筋型糖原病，肝型糖原病を400例以上診断してきた。従来本症は“糖原病”と呼称しているが，症例によってはグリコーゲンがほぼ正常あるいはグリコーゲンが逆に枯渇している疾患があることが判明し，糖原病（glycogen storage disease ; glycogenosis ; GSD）と呼ぶより，グリコーゲン代謝異常症（disorders of glycogen metabolism ; DGM）と呼ぶほうがより正確な病態を表す診断名であることを提唱した。

治療的な側面では Pompe 病に対する酵素補充療法，McArdle 病に対するビタミン B6 療法などの成果が報告され，患者の日常生活動作（ADL）の顕著な向上を認めている。またグリコーゲン合成系の異常による新たな臨床病型も発見され，グリコーゲン代謝異常症は幅広い臨床スペクトラムを呈する症候群であることがわかってきた。それに加え脳におけるグリコーゲンの役割と，脳性まひについてその発生起序について考察を加えた。

グリコーゲン代謝異常症は1929年にはじめてI型が報告されて以来様々な酵素欠損が蓄積され現在15病型になっている。古い疾患ではありながら，最近その病態，新たな酵素欠損，病型の発見が次々となされ，今後もさらに進展が期待される大変興味深い領域である。

見出し語 グリコーゲン代謝異常症，糖原病，McArdle 病，グリコーゲン合成酵素，脳代謝，アストロサイト

はじめに

筆者は主にグリコーゲンの代謝に起因する筋型糖原病，肝型糖原病を約30年にわたって診断，研究をしてきた。依頼によって検査した検体は1,500件を超え，診断できた症例も400例以上あり，その中には大変稀な疾患も含まれている。本稿では「グリコーゲン」を主題として，今までの研究を振り返ってみたい。グリコーゲン代謝異常の研究過程で，症例の病名（診断名）は“糖原病”と総称しているが，症例によってはグリコーゲンが蓄積しているというオリジナルの概念からは逸脱したものも明らかになり，グリコーゲンがほぼ正常あるいはグリコーゲンが逆に枯渇している疾患までも糖原病という範疇に入ってきた。皮膚にも糖原病0型は「glycogen storage disease without glycogen」と揶揄されるに至り，研究者は従来用いられている“糖原病”という疾患名に違和感を持つようになってきていた。そこで筆者は糖原病（glycogen storage disease ; glycogenosis ; GSD）と呼ぶより，グリコーゲン代謝異常症（disorders of glycogen metabolism ; DGM）

と呼ぶほうがより正確な病態を表す診断名であることを提唱してきた。

本稿ではこの際従来の呼称ではなく，グリコーゲン代謝異常症（disorders of glycogen metabolism ; DGM）として以下記載してゆくが，従来の“糖原病”のギリシャ数字で冠された病型については慣例としてそのまま使用することとする。

以下，(1) グリコーゲン代謝の役割，(2) グリコーゲン代謝異常症の今までの報告の特徴と経緯，(3) 新たなグリコーゲン代謝異常症と McArdle 病の治療，(4) 脳におけるグリコーゲンの役割についての考察，(5) 診断の問題点について順に述べる。

I グリコーゲン代謝の役割¹⁾

グリコーゲンは動物性の貯蔵グルコースであるが，植物では澱粉がそれに相当する。樹枝状にグルコース残基が1-4結合あるいは，1-6結合で結合している。生体では主に肝臓，筋肉に貯蔵され必要な時に glycogenolysis/glycolysis（解糖）という代謝過程で分解される（図1）。グリコーゲンの分解（解糖）は臓器によってその目的が異なっている（表1）。肝臓では貯蔵されたグリコーゲンはグルコース-6-ホスファターゼ（glucose-6-phosphatase ; G-6-Pase）の働きでグルコースへ変換され，血糖の維持に利用される。一方筋肉では解糖はエネルギー産生が目的で，嫌気であれば乳酸へ，好気の状態であればアセチル CoA を通じて TCA サイクル，呼吸鎖と進み，1

常葉大学保健医療学部

連絡先 〒431-2102 浜松市北区都田町1230

常葉大学保健医療学部（杉江秀夫）

E-mail : sugie@hm.tokoha-u.ac.jp

（受付日：2014. 12. 26）